Journal of Advanced Marine Engineering and Technology, Vol. 49, No. 5, pp. 378~384, 2025
J. Advanced Marine Engineering and Technology (JAMET)
https://doi.org/10.5916/jamet.2025.49.5.378

ISSN 2234-7925 (Print)
ISSN 2765-4796 (Online)
Original Paper

Design approach of label tags for item management Using UHF RFID

Jaeyul Choo†

(Received September 18, 2025 ; Revised September 29, 2025 ; Accepted October 2, 2025)

Abstract: This study provides guidance for the design and analysis of a practical ultra-high-frequency (UHF) radio frequency identification (RFID) label tag antenna that achieves stable readability over a range of target objects. The study discusses the fundamental aspects of power transfer, antenna architecture, and microchip packaging in RFID systems, with a specific focus on the challenges of impedance matching caused by the varying dielectric properties of adjacent materials. To overcome these obstacles, a compact tag antenna structure that integrates a T-matching loop, meander-spiral dipole, and capacitive end load was examined. The designed tag antenna was optimized using electromagnetic simulations and fabricated on a flexible polyethylene terephthalate substrate by employing flip-chip bonding processes. Experimental results showed a maximum read range of 6.3 m at 917 MHz, with consistent performance even when the substrate dielectric constant increased to 5. The proposed antenna design offers a straightforward, low-cost, and robust solution for item-level RFID deployment, enabling dependable impedance matching and enhanced readability in practical applications.

Keywords: Antenna radiation pattern, Electromagnetic numerical analysis, Far-field zone, Near-field zone, Radio frequency identification, Tag antenna

1. Introduction

Radio frequency identification (RFID) has become increasingly prevalent in various practical applications, primarily because it enables automatic identification for efficient tracking and management of objects. An RFID system consists of tags (either with or without a battery, designated as active or passive) that are attached to objects to store relevant information, and readers that extract data from these tags. Based on their operating frequency bands, RFID systems are categorized as low-frequency (LF, 125–134 kHz), high-frequency (HF, 13.56 MHz), ultra-high-frequency (UHF, 860–960 MHz), and microwave (2.4 GHz and 5.8 GHz) systems **[1]-[3]**. LF and HF RFID systems employ inductive coupling between the reader and tag antennas within the near-field zone, where performance is influenced by the geometry of both antennas. Conversely, UHF and microwave RFID systems utilize backscattered waves from the tag to the reader through the far-field zone, where both the overall antenna size and the operating frequency play critical roles in system performance **[4]-[7]**. Specifically, the passive UHF RFID system offers several advantages over systems operating in other frequency bands because it allows for the minimization of antenna size, making it suitable for item-level tagging applications that require small antennas for attachment to compact items **[2]**. Near-field communication (NFC) in the UHF band has recently been introduced to enable reliable item-level tagging and provide consistent performance despite varying environmental factors. NFC operates via inductive coupling, making use of the near magnetic flux that induces current in accordance with Faraday's law of induction **[8]**. Typically, a loop antenna is chosen for NFC because of its ability to strongly generate a near-magnetic field proportional to its perimeter, as its loop structure efficiently produces the induced current in response to the magnetic field generated by the other antenna.

For far-field communication in item-level applications within UHF RFID systems, the tag antenna plays a crucial role in mitigating performance degradation due to adjacent dielectric or metallic materials. To address this challenge, previous research has developed effective T-matching networks tailored for various dielectrics, as documented in **[9]**. The antenna introduced in this study utilizes a T-matching network consisting of a dipole with a capacitive end load and a thick-stripline T-matching structure, thereby achieving stable tag sensitivity (minimum operating power), regardless of the dielectric characteristics of the attached material. Nonetheless, the proposed label tag exhibits limitations,

† Corresponding Author (ORCID: http:// orcid.org/0000-0002-5804-858X): Associate Professor, School of Electronics & Mechanical Engineering, Gyeongkuk National University, 1375, Gyengdong-ro, Andong 36729, Korea, E-mail: jychoo@gknu.ac.kr, Tel: 054-820-5424

as it does not perform adequately on metallic surfaces owing to significant changes in key antenna properties, including operating frequency, radiation efficiency, radiation pattern, and input impedance. As an alternative method, metal-compatible tags incorporating an embedded ground plane have been introduced **[10]-[12]**. These antennas demonstrate reliable operation on a variety of dielectric and metallic surfaces as the integrated ground plane effectively isolates the antenna from the influence of underlying materials. However, the configuration's rigid, voluminous, and intricate design, attributable to the ground plane, restricts their suitability for flexible substrates such as textiles and liquids and leads to increased manufacturing costs and complexity, which is a drawback for large-scale production. Thus, it is necessary to develop a versatile tag suitable for both dielectric and metallic environments.

In this paper, we first introduce the operating principle of tags, including a microchip and a reader, in the UHF RFID system. We then explain the impedance matching between a tag antenna and a microchip, considering flip-chip bonding effects. Finally, we introduce a tag antenna that maintains stable reading performance across a variety of dielectric materials.

2. Basic Theory of RFID Tags in the UHF Band

2.1 Power Transfer

Identification in RFID systems is principally determined by the power transfer from the reader to the tag equipped with a microchip. The overall readability of the system depends on the performance of the tag, because the minimum detectable power (reader sensitivity) is generally much lower than that required by the tag.

Figure 1 illustrates the power transfer process from the reader to the tag, with the parameters and equations defined as follows:

- Transmitting power of the reader (W): $P_{t,reader}$
- Received power of the reader (W): $P_{r,reader}$
- Distance between tag and reader (m): R
- Transmitting power of the tag (W): $P_{t,tag}$
- Received power of the tag (W): $P_{r,tag}$
- Received power of the chip (W): $P_{r,chip}$
- Induced current from the tag antenna (A): $I_{r,tag}$
- Voltage at the antenna (V): $V_{r,tag}$
- Voltage in the chip (V): $V_{r,chip}$
- Impedance of the chip (Ω): Z_{chip}
- Impedance of the tag antenna (Ω): Z_{ant}
- Total gain of the reader antenna: G_{reader}

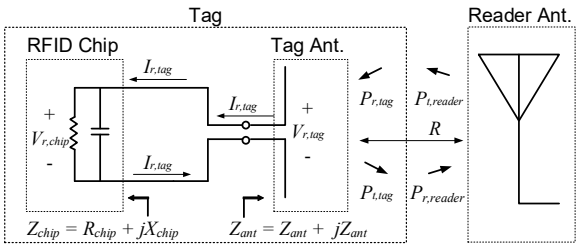

Figure 1: Illustration of power transfer between the reader and the tag

- Total gain of the tag antenna: G_{ant}

$$P_{r,tag} = P_{t,reader}\frac{G_{ant}G_{reader}\lambda^2}{(4\pi R)^2} = \frac{1}{2}\left[V_{r,tag} \times {I_{r,tag}}^*\right] = \frac{1}{2}V_{r,tag}\left[\frac{{V_{r,tag}}^*}{R_{chip}+R_{ant}}\right] \quad (1)$$

$$P_{r,chip} = \frac{1}{2}\left[V_{r,chip} \times {I_{r,chip}}^*\right] = \frac{1}{2}\left|V_{r,chip}\right|^2\left[\frac{1}{Z_{chip}}\right] = \frac{1}{2}\left|V_{r,tag}\right|^2\left|\frac{Z_{chip}}{Z_{ant.}+Z_{chip}}\right|^2\left[\frac{1}{Z_{chip}}\right] = \frac{1}{2}\left|V_{r,tag}\right|^2\frac{R_{chip}}{(R_{ant.}+R_{chip})^2+(X_{ant.}+X_{chip})^2} = \frac{1}{2}P_{r,tag}\left(1-\eta_{tag}^2\right) \quad (2)$$

$$P_{r,Chip(max)} = \frac{1}{8}\frac{\left|V_{r,tag}\right|^2}{R_{tag}} = \frac{1}{2}P_{r,tag} \quad (3)$$

where $\eta_{tag} = \frac{Z_{ant.}-Z^*_{chip}}{Z_{ant.}+Z_{chip}}$

In a free-space propagation environment, the power received by a tag antenna ($P_{r,tag}$) can be determined using the Friis free-space equation, as given in (1) [13]. The received power at the tag induces a current ($I_{r,tag}$), which, in turn, activates the charge capacitor in the microchip, enabling the microchip to operate. Specifically, the received power delivered to the chip ($P_{r,chip}$), which is described by **Equation (1)–(3)**, achieves a maximum value equal to half of $P_{r,tag}$ under the conjugate matching condition ($R_{chip} = R_{ant}$ and $X_{chip} = -X_{ant.}$).

2.2 Tag Antennas

Early commercial RFID tags primarily used planar loop and microstrip dipole antennas. In particular, the dipole (or ground-backed monopole) antenna has remained prevalent in various wireless applications owing to its omnidirectional radiation pattern, straightforward geometry, easy control of the input

Table 1: Tag characteristics according to feeding type.

	Matching method (Feeder)		
	Direct connection feed	Inductive coupling feed	T-type matching feed
Read stability	Low	Normal	High
Q-factor	High	Low	Low
Bandwidth	Narrow	Broad	Broad

impedance, and comparatively compact size. Nevertheless, these antennas are limited by their narrow bandwidth and variation in input impedance near adjacent objects owing to their high-quality (Q) factor. To address these issues, various electrical techniques, such as inductively coupled matching, capacitively coupled matching, and single and double T-matching, have been adopted. **Table 1** provides a comparison of the characteristics of developed RFID tags **[14]-[17]**.

2.3 Microchip

Microchips are released by the manufacturers using the Generation 2 protocol. Although the same protocol is applied, the terminal characteristics of the microchips differ across manufacturers. Furthermore, the number of antenna ports, terminal impedances, and memory structures is determined by each company. An RFID tag integrates both a microchip and an antenna into a compact package designed such that the microchip can be attached directly to the antenna. High packaging throughput significantly reduces transponder costs. Consequently, flip-chip bonding is generally preferred to wire bonding.

Figure 2 illustrates the bonding region between the RFID tag antenna and the microchip, as viewed with a scanning electron microscope (SEM), and the corresponding schematic configuration **[18]**. Specifically, **Figures 2(a)** and **(b)** show the conductive pads connected to an antenna trace etched in an aluminum layer on a dielectric substrate such as polyethylene terephthalate (PET). The microchip consists of a silicon layer for the chip circuit and bumps as the terminals. The microchip communicates with the antenna via the conductive ball of an electrically conductive adhesive between the bumps and the antenna pads. Consequently, the information stored in the microchip can be transmitted to the reader via the electrical connection of the bonding joint.

The bonded region is also modeled using the equivalent circuit depicted in **Figure 3**. **Figure 3** shows the impedance (Z_{pkg}) of the packaged chip, which includes the parasitic impedance ($Z_{par.}$), determined by both the bump height and internal pattern of the microchip. Since the parasitic impedance significantly impacts the impedance matching with the tag antenna, careful consideration of geometrical parameters is essential for ensuring the reliability of RFID tag production. Furthermore, the chip impedance (Z_{chip}) should be regarded as equally important as the parasitic impedance, because the quality factor (Q factor) of the chip impedance (X_{chip} / R_{chip}) determines the feasible range of antenna impedance for achieving conjugate matching. **Figure 4** illustrates the received power of a tag as a function of the antenna impedance normalized by the resistance and reactance of the microchip, respectively. By targeting the received power within the -3 dB design goal, the antenna can be designed to be approximately within the range of $R_{n,ant.}$ ($0.2R_{chip} < R_{ant.} < 5.8R_{chip}$) for resistance, and $X_{n,ant.}$ ($0.72QR_{chip} < X_{ant.} < 1.28QX_{chip}$) for reactance.

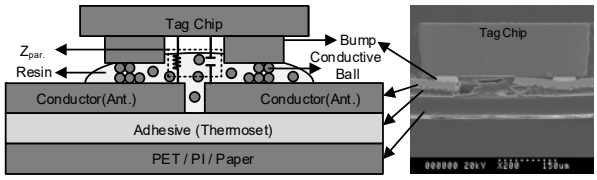

(a) (b)

Figure 2: Cross-section of the bonded microchip region. (a) Structure of flip chip bonding. (b) SEM cross-sectional image of the bonded microchip

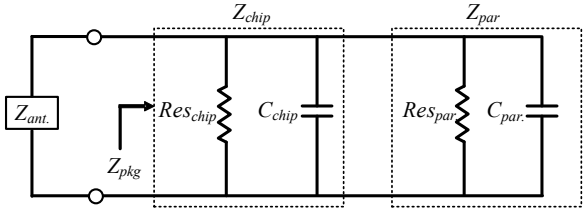

Figure 3: Equivalent circuit model of the bonded region

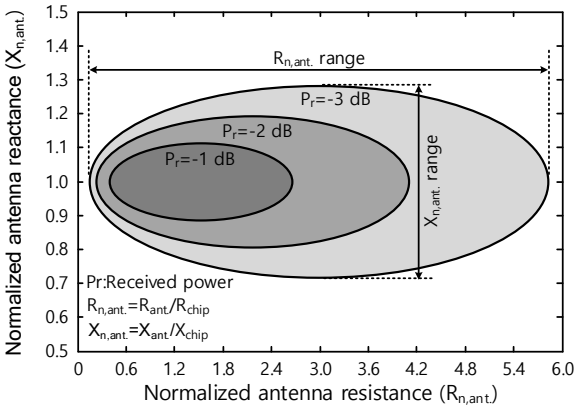

Figure 4: Impedance-matching characteristics of the tags

Therefore, a higher Q factor in the microchip enables the antenna to maintain stable performance despite the presence of unwanted parasitic impedance.

3. T-matching Label Tags

Recently, achieving impedance matching with microchips has become a challenge in the design of UHF RFID tags. In addition to inductively coupled matching, the T-matching technique is considered an effective and practical approach for attaining good matching characteristics with a capacitive microchip. Several studies have analyzed T-matching in detail **[9]-[10]**, **[16]-[17]**. As a geometric approach, **[9]** introduces an optimal geometry for the T-matching loop to achieve consistent readability even in proximity to various materials. A longitudinally narrow T-matching loop allows the tag antenna to counteract electrical variations caused by shifts in the effective wavelength when placed on different dielectric substrates. This consistent electrical performance of the tag antenna contributes to stable reading regardless of nearby objects.

Building on previous work on T-matching, we introduced a slim label-type tag antenna designed for consistent readability in proximity to various dielectric materials **[19]**. The introduced tag antenna integrates a T-matching loop with a meander-spiral dipole featuring a capacitive end load. The geometry of the antenna was optimized to interface with a commercial chip exhibiting a measured impedance of Z_{chip} = 13 − j163 Ω and a minimum operating power of -15 dBm at 912 MHz **[9]**. The overall structure of the antenna, measuring 70 mm × 6 mm, was fabricated on a PET substrate (ε_r = 4, tanδ = 0.003, and thickness = 50 μm), which served as a flexible substrate. During the design process, we considered embedding the printed tag in a thin polymer film (PET, ε_r = 4.5, tanδ = 0.001, and thickness = 0.4 mm) to account for the potential shift in the operating frequency due to packaging. To predict performance, we rigorously calculated the maximum reading range (R_{max}) based on **Equation (1)-(3)**, considering the antenna impedance (Z_{ant}), radiation efficiency (η), and directivity (D) obtained from high-frequency structure simulator (HFSS), a commercial electromagnetic field simulator **[20]**.

The overall configuration and parameters of the proposed antenna are shown in **Figure 5**. The design comprises a T-matching loop and a meander-spiral dipole directly connected to the capacitive end load. The inner perimeter ($2H_1$+$2V_2$) of the T-matching loop predominantly determines the inductance required for optimal matching with the microchip. The ratios V_2 / V_1 and V_3 / V_1

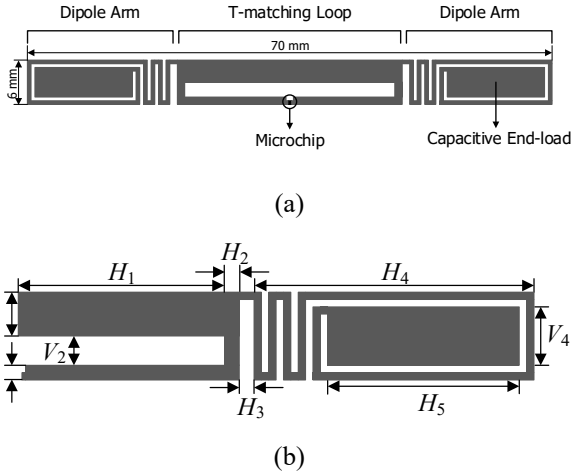

Figure 5: Structure of the introduced tag antenna. (a) Components of the tag antenna. (b) Specification of design parameters.

are critical as they dictate the current division factor, thereby influencing the distribution of the current between the dipole arms and the T-matching loop **[13]**. The meander-spiral dipole enables precise control over the capacitance and inductance, in addition to tuning the overall electrical length for the targeted operating frequency. Moreover, the capacitive end load plays a crucial role in broadening the matching bandwidth. Therefore, optimizing these design parameters is essential for achieving an effective antenna structure and impedance matching.

To design an optimal antenna, we conducted a parametric study focusing on a T-matching loop and a meander-spiral dipole. **Figure 6** presents the simulated antenna impedance as V_2 and V_3 vary, while V_1 and H_1 are set at 1.1 mm and 14 mm, respectively.

The dotted line indicates the conjugate impedance of the microchip. As V_2 increased from 1 to 3 mm, the self-resonance frequency shifted to a lower frequency range. By considering the difference between the maximum and minimum values, the tunable impedance range can be determined using both the V_2 / V_1 and V_3 / V_1 ratios, as anticipated. Additionally, we analyzed the changes in the antenna impedance by modifying the capacitive end load of the meander-spiral dipole. Extending the spiral length resulted in a downward shift in the self-resonance frequency [19]. Notably, geometric adjustments to the T-matching loop and meander-spiral arms readily achieve impedance matching while largely preserving the antenna pattern. Based on this comprehensive parametric analysis, we selected optimized design parameters to ensure a consistent reading range. The finalized parameters are as follows: V_1 = 1.1 mm, V_2 = 2 mm, V_3 = 2.9 mm, V_4 = 4 mm, H_1 = 14 mm, H_2 = 1 mm, H_3 = 1 mm, H_4 = 19 mm, H_5 =

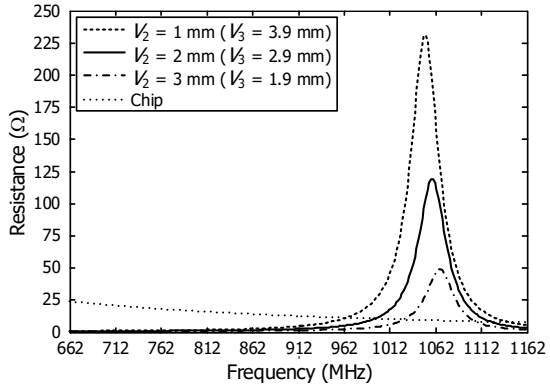

(a)

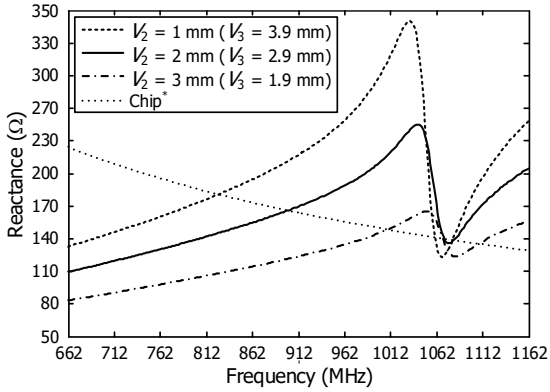

(b)

Figure 6: Antenna input impedance for different T-matching loop values. (a) Resistance. (b) Reactance.

13 mm, with meander and spiral line width and spacing set at 0.5 mm.

An optimal label tag with a bonded microchip was fabricated using flip-chip bonding and packaging techniques. The reading performance of the introduced tag was evaluated by measuring the tag sensitivity ($P_{tag\,min.}$), which represents the minimum operating power of the tags, and calculating the reading range (R_{read}) based on **Equation (4)** and **(5) [10]**.

$$P_{tagmin.} = \frac{P_{chipmin}}{(1-\eta_{tag}^2)Eff_{tag}D_{tag}}$$

$$= \frac{P_{min}(1-\eta_{reader}^2)Eff_{reader}D_{reader}}{\left(R_{fixed}\frac{4\pi}{\lambda}\right)^2} \quad (4)$$

$$R_{read} = \frac{\lambda}{4\pi}\sqrt[\frac{\lambda}{4\pi}]{\frac{EIRP}{P_{tagmin.}}}\sqrt{\frac{P_T(1-\eta_{reader}^2)Eff_{reader}D_{reader}}{P_{tagmin.}}}$$

where η *Eff*, *D*, and R_{fixed} are the return loss, radiation efficiency, directivity, and fixed distance (1 m) between the reader antenna and the tag, respectively.

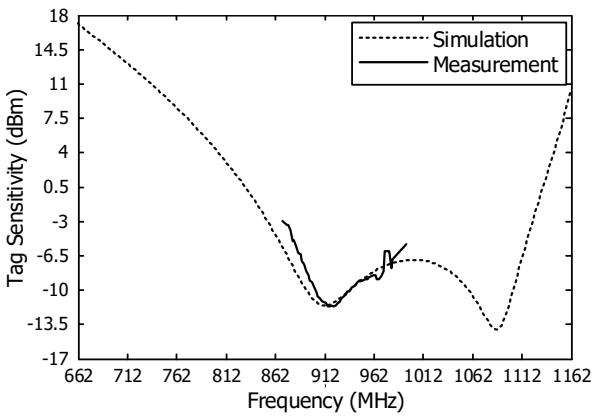

(a)

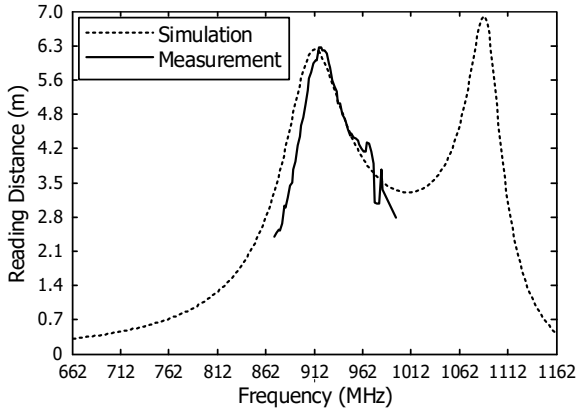

(b)

Figure 7: Reading performance. (a) Tag sensitivity. (b) Reading range

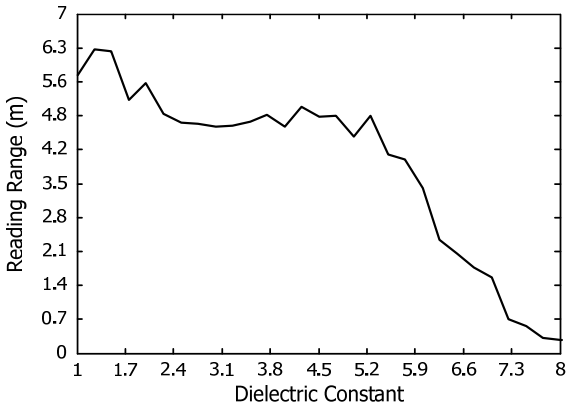

Figure 8: Reading range of the introduced tag as a function of the dielectric constant of the underlying material

We first measured the tag sensitivity of the attached tag on an air-like foam substrate using Tagformance Lite (Voyantic Corporation), as depicted in **Figure 7(a) [21]**. Furthermore, the reading range was estimated using the measured tag sensitivity under a

36 dBm EIRP (6 dB linear polarization), as shown in **Figure 7(b)**.

The tag sensitivity exhibited a minimum value of -11.7 dB at 917 MHz, which corresponded to a maximum reading range of 6.3 m. **Figure 7** confirms that measurements generally correspond well with simulated results, with the only notable discrepancy being a frequency shift of approximately 5 MHz. This discrepancy between the simulation and the measurement likely arose from the antenna impedance being affected by the supporting foam, which was assumed to be an air substrate in the simulation.

For applications requiring the detection of only a single object in RFID systems, tag antennas are typically designed with a focus on the characteristics of a specific target object. However, for a more general tag usage across a variety of applications, the antenna design must ensure robust impedance matching over diverse target objects. Therefore, we evaluated the reading range of the introduced tag as greater than 4 m when the dielectric constant of the underlying material (thickness = 5 mm) ranged from 1 to 8. **Figure 8** shows the measured reading range at 912 MHz for tags attached to objects with dielectric constants ranging from 1 to 8. The reading range remained stable when the dielectric constant (ε_r) was between 1 and 5, but decreased when the dielectric constant (ε_r) exceeded 5. These findings demonstrate that effective impedance matching between the microchip and tag antenna persists for dielectric constants less than 5. In summary, the T-matching configuration offers a straightforward solution for achieving reliable impedance matching across various target objects in RFID applications.

4. Conclusion

This study reviews the operational principles of UHF RFID systems and introduces a compact and flexible label tag antenna engineered for stable performance across various target objects. By integrating a T-matching loop and a meander-spiral dipole with capacitive loading, the introduced design achieved effective impedance matching with standard RFID chips, even when applied to substrates with different dielectric properties. The test results showed a maximum reading distance of 6.3 m and consistently reliable operation for materials with dielectric constants of up to 5. These findings suggest that the proposed tag-antenna design represents a practical, cost-efficient, and scalable solution for UHF RFID item-level tagging, thus facilitating improved asset management and tracking in a wide range of environments.

Acknowledgement

This work was supported by a Research Grant of Gyeongkuk National University.

Author Contributions

Conceptualization, J. Choo; Methodology, J. Choo; Software, J. Choo; Validation, J. Choo; Formal Analysis, J. Choo; Investigation, J. Choo; Resources, J. Choo; Data Curation, J. Choo; Writing—Original Draft Preparation, J. Choo; Writing—Review & Editing, J. Choo; Visualization, J. Choo; Supervision, J. Choo; Project Administration, J. Choo; Funding Acquisition, J. Choo.

References

[1] K. Finkenzeller, RFID Handbook: Radio-frequency Identification Fundamentals and Applications, 2nd ed: Wiley, 2004.

[2] P. V. Nikitin, K. V. S. Rao, and S. Lazar, “An overview of near field UHF RFID,” IEEE International Conference on RFID, pp. 167-174, 2007.

[3] K. V. S. Rao, P. V. Nikitin, and S. F. Lam, “Antenna design for UHF RFID tags: a review and a practical application.” IEEE Transactions on Antennas and Propagation, vol. 53, no. 12, pp. 3870-3876, 2005.

[4] R. Harrington, “On the gain and beamwidth of directional antenna.” IEEE Transactions on Antennas and Propagation, vol. 6, no. 3, pp. 219-225, 1958.

[5] J. S. Mclean, “A re-examination of the fundamental limits on the radiation Q of electrically small antenna,” IEEE Transactions on Antennas and Propagation, vol. 44, no. 5, pp. 672-676, 1996.

[6] C. Cho, H. Choo, and H. Ling, “Design of small tag antennas for RFID application,” 2004 Korea-Japan Joint Conference on AP/EMC/EMT, pp. 27-31, 2004.

[7] C. Cho, H. Choo, and I. Park, “Design of UHF small passive tag antennas,” Antennas and Propagation Society International Symposium, vol. 2B, pp. 349-352, 2005.

[8] D. K. Cheng, Fundamentals of Engineering Electromagnetics, Addison-Wesley, 1993.

[9] J. Choo, J. Ryoo, J. Hong, C. Choi, and M. Tentzeris, “T-matching networks for the efficient matching of practical RFID tags,” 39th European Microwave Conference, pp. 5-8, 2009.

[10] J. Choo and J. Ryoo, “UHF RFID tag applicable to various objects,” IEEE Transactions on Antennas and Propagation, vol. 62, no. 2, pp. 922-925, 2014.

[11] L. Mo, H. Zhang, and H. Zhou, “Broadband UHF RFID tag antenna with a pair of U slots mountable on metallic objects,” Electronics Letters, vol. 44, no. 20, pp. 1173-1774, 2008.

[12] C. Cho, H. Choo, and I. Park, “Design of planar RFID tag antenna for metallic objects,” Electronics Letters, vol. 44, no. 3, pp. 175-177, 2008.

[13] C. A. Balanis, Antenna theory analysis and design, 4th ed, John Wiley & Sons, 1997.

[14] C. Choo and H. Ling, “Design of electrically small planar antennas using inductively coupled feed,” Electronics Letters, vol. 39, pp. 1563-1565, 2003.

[15] C. C. Chang and Y. C. Lo, “Broadband RFID tag antenna with capacitively coupled structure,” Electronics Letters, vol. 42, pp. 1322-1323, 2006.

[16] C. Cho, H. Choo, and I. Park, “Design of planar RFID tag antenna for metallic objects,” Electronics Letters, vol. 44, pp. 175-177, 2008.

[17] C. Cho, H. Choo, and I. Park, “Broadband RFID tag antenna with quasi-isotropic radiation pattern,” Electronics Letters, vol. 41, pp. 1091-1092, 2005.

[18] J. Choo and J. Ryoo, “Analysis of flip chip bonding for performance,” IEEE Transactions on Components, Packaging and Manufacturing Technology, vol. 4, no. 10, pp. 1714–1721, 2014.

[19] J. Choo, C. Cho, and H. Choo, “Three label tags for special applications: attaching on small targets, long distance recognition, and stable performance with arbitrary objects,” IEICE Transactions on Communications, vol. E97-B, no. 5, 2014.

[20] Ansys HFSS. [Online]. Available: http://www.ansys.com

[21] Tagformance Lite. [Online]. Available: http://www.voyantic.com.